

## Investigation into the temperature dependence of isotropic- nematic phase transition of Gay- Berne liquid crystals

A Avazpour and S M Hekmatzadeh

Department of Physics, Yasouj University, Yasouj, Iran  
E-mail: avazpour@yu.ac.ir

(Received 8 September 2013 , in final from 06 August 2014)

### Abstract

Density functional approach was used to study the isotropic- nematic (I-N) transition and calculate the values of freezing parameters of the Gay- Berne liquid crystal model. New direct and pair correlation functions of a molecular fluid with Gay- Berne pair potential were used. These new functions were used in density functional theory as input to calculate the isotropic- nematic transition densities for elongation  $x_0 = 3.0$  at various reduced temperatures. It was observed that the isotropic- nematic transition densities increase as the temperature increases. It was found that the new direct correlation function is suitable to study the isotropic- nematic transition of Gay- Berne liquids. Comparison to other works showed qualitative agreement.

**Keywords:** Gay- Berne potential, direct correlation function, density functional theory, isotropic- nematic transition

### 1. Introduction

Liquid crystal state is a distinct phase of matter observed between crystalline (solid) and isotropic (liquid) states. There are many types of liquid crystal states, which depend on the degree of material order. The liquid crystals are anisotropic materials, the physical properties of which vary with the average alignment of molecules with director [1]. High alignment results in a very anisotropic material while the low alignment gives an almost isotropic material. The nematic phase of liquid crystal is distinguished by molecules that have no positional order while tending to be directed along the director. The smectic state is another distinct mesophase of liquid crystal substances. In this phase, the molecules show a degree of translational order, which is not present in the nematic phase. In the smectic state, the molecules not only keep the general orientational order of nematics, but also tend to be aligned in layers or planes [1- 3]. The liquid crystal with cholesteric (or chiral nematic) phase is typically composed of nematic mesogenic molecules containing a chiral center which produces intermolecular forces aligning molecules with a small angle between them. Columnar liquid crystals are different from the above-mentioned types in terms of their shape. They are disc-shaped while others are long rods in shape. This mesophase is distinguished by the stacked columns of molecules.

Intermolecular interactions are responsible for the existence of liquids and solids in nature. They determine the physical and chemical properties of gases, liquids and crystals in addition to the stability of chemical complexes and biological compounds [4]. There are limited accurate theoretical potentials available for polyatomic molecules. Therefore, statistical-mechanical calculations are usually done with model potentials [5]. Despite their simplicity, hard or soft repulsive ellipsoids are not best suited for the study of generic liquid crystal properties. For example, such models do not exhibit smectic phases. Furthermore, one cannot study the effect of attractive interactions, the interplay between liquid-crystalline order and liquid-vapor phase separation, etc. A model, closer to real mesogenic systems, explicitly considers anisotropic short-range repulsive as well as long-range attractive interactions. Along with this, Berne and Pechukas proposed a Gaussian overlap potential model [6]. This potential was used to model the liquid crystal. However, it suffers from some unrealistic features, as noticed by Gay and Berne (GB) [7]. They introduced a class of ellipsoidal pair potentials with attractive interactions, which has become one of the standard liquid crystal potentials [8].

A realistic pair-potential between nonspherical molecules is fairly complex. To our knowledge about the Lennard- Jones fluids, much can be learned about system

of nonspherical molecules from the GB potential [9]. The intermolecular pair-potential proposed by Gay and Berne is written as

$$U(1,2) = U(\hat{u}_1, \hat{u}_2, \hat{r}) \\ = 4\varepsilon(\hat{u}_1, \hat{u}_2, \hat{r}) \left\{ \left[ \frac{\sigma_0}{r - \sigma(\hat{u}_1, \hat{u}_2, \hat{r}) + \sigma_0} \right]^{12} - \left[ \frac{\sigma_0}{r - \sigma(\hat{u}_1, \hat{u}_2, \hat{r}) + \sigma_0} \right]^6 \right\} \quad (1)$$

where  $\hat{u}_i$  is the axial vector of molecule  $i$  and  $\hat{r}$  is a unit vector along  $\vec{r} = \vec{r}_2 - \vec{r}_1$ ,  $\vec{r}_1$  and  $\vec{r}_2$  are the center of mass positions of molecules 1 and 2, respectively.  $\varepsilon(\hat{u}_1, \hat{u}_2, \hat{r})$  and  $\sigma(\hat{u}_1, \hat{u}_2, \hat{r})$  are strength-parameters and orientation-dependent range, respectively, which are defined as:

$$\sigma_0 \left\{ 1 - \frac{1}{2} \chi \left[ \frac{(\hat{u}_1 \cdot \hat{r} + \hat{u}_2 \cdot \hat{r})^2}{1 + \chi(\hat{u}_1 \cdot \hat{u}_2)} + \frac{(\hat{u}_1 \cdot \hat{r} - \hat{u}_2 \cdot \hat{r})^2}{1 - \chi(\hat{u}_1 \cdot \hat{u}_2)} \right] \right\}^{-\frac{1}{2}} \quad (2)$$

$$\varepsilon(\hat{u}_1, \hat{u}_2, \hat{r}) = \varepsilon_0 \varepsilon^\nu(\hat{u}_1, \hat{u}_2) \varepsilon'^\mu(\hat{u}_1, \hat{u}_2, \hat{r}), \quad (3)$$

where

$$\varepsilon(\hat{u}_1, \hat{u}_2) = \left[ 1 - \chi^2 (\hat{u}_1 \cdot \hat{u}_2)^2 \right]^{-\frac{1}{2}}, \quad (4)$$

and

$$\varepsilon'(\hat{u}_1, \hat{u}_2, \hat{r}) = 1 - \frac{1}{2} \chi' \left[ \frac{(\hat{u}_1 \cdot \hat{r} + \hat{u}_2 \cdot \hat{r})^2}{1 + \chi(\hat{u}_1 \cdot \hat{u}_2)} + \frac{(\hat{u}_1 \cdot \hat{r} - \hat{u}_2 \cdot \hat{r})^2}{1 - \chi(\hat{u}_1 \cdot \hat{u}_2)} \right], \quad (5)$$

with

$$\chi = \frac{(k^2 - 1)}{(k^2 + 1)} \text{ and } \chi' = \frac{\left( \frac{1}{k'^\mu} - 1 \right)}{\left( \frac{1}{k'^\mu} + 1 \right)}, \quad (6)$$

and  $k$  is the ratio of molecular length to breadth which is equal to 3 for the system considered here and  $k'$  is the ratio of the potential well depths for the side-by-side and end-to-end configurations of the molecules. Also, the two adjustable parameters  $\mu$  and  $\nu$  control anisotropy in the interaction potential. Note that the GB potential, eq. (1), reduces to the spherical Lennard-Jones potential when both  $k$  and  $k'$  are equal to unity. The exact form of the GB potential is determined by using four parameters  $k$ ,  $k'$ ,  $\mu$  and  $\nu$ . Four basic configurations can be defined for the potential between two GB particles [10]. In the side-by-side configuration, the symmetry axes of the pairs of molecules are parallel. The vector joining the center of masses is perpendicular to

these symmetry axes, while they are parallel in the end-to-end configuration. In T configuration, one symmetry axis is parallel to the vector joining the center of masses while the other is perpendicular to both. The last configuration is cross-configuration ( $\times$ ) in which the symmetry axes and the vector between centers of masses are perpendicular.

The results obtained from computer simulation [11-13] show that the GB potential is capable of forming nematic, smectic A, smectic B, and an ordered solid in addition to the isotropic liquid. A variety of mesophases, formed by the anisotropic molecules interacting via the GB potential, are of high interest. Taking the attractive forces into account in the molecular model makes the phase diagram a little more realistic. Thus the GB potential has become a standard model for studying liquid crystal phases [9, 14, 15].

Some theoretical attempts have also been made to calculate the GB phase diagram using density functional theory (DFT), perturbation methods and virial approximations [16 - 19]. The DFT has been used to study freezing of liquid crystals [20] and confined hard and soft ellipsoids [21, 22]. In addition to phase behavior of the GB mesogen, many other aspects such as the behavior of solute molecules in a GB solvent [23], elastic constants [24, 25], viscosity coefficients [26, 27], thermal conductivity [28] and the behavior in confining geometries [29] have been studied. The exponents  $\mu$  and  $\nu$  define different variants of the potential. The most studied and widely used parameterizations are given in ref. [30].

In this paper, we test the accuracy of a new direct correlation function (DCF) for GB molecules by using DFT for freezing of molecular liquids [9]. We also study the isotropic - nematic transition (the orientational freezing) of GB molecules. Following the work of Singh *et al.* [9, 31, 32], here, we investigate, the effect of varying  $T^* = k_B T / \varepsilon_0$  on the properties of molecular liquids. This paper is organized as follows. In section 2, the theory is outlined. In section 3, the new DCF is introduced. In section 4, the new pair distribution function ( $g(r, \hat{\Omega}_1, \hat{\Omega}_2)$ ) is introduced and finally, in section 5, the numerical calculations and results are discussed.

## 2. Grand thermodynamic potential

The grand thermodynamic potential difference between ordered and isotropic phases is written as [32]

$$\Delta W = W - W_f = \Delta W_1 + \Delta W_2, \quad (7)$$

where  $W$  and  $W_f$  are the grand thermodynamic potential of ordered and isotropic phases, respectively.

The entropy term  $\frac{\Delta W_1}{N}$  and the interaction term  $\frac{\Delta W_2}{N}$ , as a functional of the ordered phase singlet distribution,  $\rho(\vec{r}, \Omega)$ , are written as

$$\frac{\Delta W_1}{N} = \frac{1}{\rho_f V} \int d\vec{r} d\Omega \left[ \rho(\vec{r}, \omega) \ln \left( \frac{\rho(\vec{r}, \omega)}{\rho_f} \right) - \Delta \rho(\vec{r}, \omega) \right], \quad (8)$$

and

$$\frac{\Delta W_2}{N} = -\frac{1}{2\rho_f V} \int d\vec{r} d\Omega_1 d\Omega_2 \Delta \rho(\vec{r}_1, \Omega_1) C(\vec{r}, \Omega_1, \Omega_2) \Delta \rho(\vec{r}_2, \Omega_2), \quad (9)$$

where  $\rho_f$ ,  $V$  and  $C(\vec{r}, \Omega_1, \Omega_2)$  are number density, system volume and direct correlation function of isotropic liquid, respectively. Here,  $\Delta \rho(\vec{r}, \Omega) = \rho(\vec{r}, \Omega) - \rho_f$ . The density of ordered phase can be obtained by minimizing eq. (7) with respect to arbitrary variation in the ordered phase density subject to the constraint that there is one molecule per lattice site (for perfect crystal) and orientational distribution is normalized to unit. Thus

$$\ln[\rho(\vec{r}_1, \Omega_1)/\rho_f] = \lambda_L + \int d\vec{r}_2 d\Omega_2 C(\vec{r}_1, \Omega_1, \Omega_2; \rho_f) \Delta \rho(\vec{r}_2, \Omega_2), \quad (10)$$

where  $\lambda_L$  is a Lagrange multiplier which appears in the equation due to constraint imposed on the minimization [9, 31]. For locating transition, one attempts to find the solution  $\rho(\vec{r}, \Omega)$  from eq. (10) which has the symmetry of ordered phase. For liquid densities less than a certain value  $\rho'$ , the only solution is  $\rho(\vec{r}, \Omega) = \rho_f$ . Above  $\rho'$ , a new solution is obtained which corresponds to the ordered phase. The phase with lowest grand potential is taken as stable phase. The transition point is determined by applying  $\Delta W = 0$  [9, 32]. For the molecules with axial symmetry, the singlet density of the nematic phase can be expressed as

$$\rho(\vec{r}, \Omega) = \rho_n f(\Omega), \quad (11)$$

with

$$\rho_n = \rho_f (1 + \Delta \rho^*), \quad (12)$$

where  $\Delta \rho^* = (\rho_n - \rho_f)/\rho_f$  is the relative change in the density at the transition point and  $\rho_n$  is the number density of the nematic phase.

For uniaxial nematic phase, orientation distribution function is given as

$$f(\Omega) = A_0 \exp \left[ \sum_l \lambda_l P_l(\cos \theta) \right], \quad (13)$$

which depends only on the angle  $\theta$ , between the director and the molecular symmetry axis.

$P_l(\cos \theta)$  denotes a Legendre polynomial and  $\lambda_l$  is expansion coefficient. The orientational singlet distribution is normalized to unity and  $A_0$  is determined

from the normalization condition [32].

In space- fixed frame, we can expand  $C(\vec{r}, \Omega_1, \Omega_2)$  in terms of spherical harmonics as

$$C(\vec{r}, \Omega_1, \Omega_2) = \sum_{l_1 l_2} \sum_{m_1 m_2} C_{l_1 l_2}(r) C_g(l_1 l_2; m_1 m_2 m) Y_{l_1 m_1}(\Omega_1) Y_{l_2 m_2}(\Omega_2) Y_{lm}^*(\hat{r}), \quad (14)$$

where  $C_g(l_1 l_2; m_1 m_2 m)$  and  $Y_{l m_i}(\Omega_i)$  are Clebsch - Gordan coefficients and the spherical harmonics, respectively. From eqs. (10), (13) and (14), one can express the order parameters as [31]

$$(1 + \Delta \rho^*) \delta_{l0} + \bar{P}_l = \int d\Omega_1 P_l(\cos \theta_1) \exp[\text{Sum}], \quad (15)$$

with

$$\text{Sum} = \lambda_L + \rho_f \sum_{l_1 l_2} \left[ \frac{(2l_1 + 1)(2l_2 + 1)}{2} \right] C_g(l_1 l_2 0; 000) P_l(\cos \theta_1) \bar{P}_l \int dr r^2 C_{l_1 l_2 0}(r), \quad (16)$$

where  $\bar{P}_l$  is the order parameter. The structural parameters for the nematic phase are defined as [32]

$$\hat{C}_{l_1 l_2}^0 = (2l_1 + 1)(2l_2 + 1) \rho_f \int d\vec{r} d\Omega_1 d\Omega_2 C(\vec{r}, \Omega_1, \Omega_2) P_{l_1}(\cos \theta_1) P_{l_2}(\cos \theta_2). \quad (17)$$

Using eq. (14) and after simplification, eq. (17) can be written as

$$\hat{C}_{l_1 l_2}^0 = \left[ \frac{(2l_1 + 1)(2l_2 + 1)}{4\pi} \right]^2 \rho_f C_g(l_1 l_2 0; 000) \int dr r^2 C_{l_1 l_2 0}(r). \quad (18)$$

The term of entropy in eq. (7) can be reduced to

$$\frac{\Delta W_1}{N} = -\Delta \rho^* + \frac{\rho_n}{\rho_f} \left\{ \ln \left[ \frac{\rho_n A_0}{\rho_f} + \sum_{l \geq 2} \lambda_l \bar{P}_l \right] \right\}. \quad (19)$$

The interaction term  $\frac{\Delta W_2}{N}$  is evaluated using eqs. (11) and (13),

$$\frac{\Delta W_2}{N} = -\frac{1}{2} \Delta \rho^{*2} \hat{C}_{00}^0 - \frac{(1 + \Delta \rho^*)}{2} \sum_{l_1, l_2 \geq 2} \bar{P}_{l_1} \bar{P}_{l_2} \hat{C}_{l_1 l_2}^0. \quad (20)$$

The ordered phase (translationally and/or orientationally) coexists with the isotropic liquid when

$$\left( \frac{\partial}{\partial \xi_i} \right) (\Delta W/N) = 0, \quad (21)$$

and

$$\frac{\Delta W}{N} = 0, \quad (22)$$

where  $\xi_i$ 's are variational parameters appropriate for the phase under investigation [9, 31, 32]. eqs. (21) and (22)

show a stability condition and a phase coexistence condition. The DFT calculations are done by minimizing eq. (7) with respect to the variation parameters,  $\rho_n$ ,  $\lambda_2$  and  $\lambda_4$ . The coexistence point is then located by varying  $\rho_f$  with  $\frac{\Delta W}{N} = 0$ .

### 3. Pair correlation function

The single- particle density of uniform fluid is equal to the overall number density [33]:

$$\rho_n^{(1)}(\vec{r}) = \frac{N}{V} = \rho. \quad (23)$$

Hence, the pair density of ideal gas is [33]:

$$\rho_n^{(2)}(\vec{r}) = \rho^2 \left(1 - \frac{1}{N}\right). \quad (24)$$

The appearance of the term  $\frac{1}{N}$  in eq. (24) reflects the fact that in a system containing a fixed number of particles, the probability of finding a particle in the volume element  $d\vec{r}_1$  given that another particle is in element  $d\vec{r}_2$  is proportional to  $\frac{(N-1)}{V}$  rather than  $\rho$ .

The  $n$ - particle distribution function  $g_N^{(n)}(r^n)$  is defined in terms of the corresponding particle densities by [33]

$$g_N^{(n)}(\vec{r}^n) = \frac{\rho_N^{(n)}(\vec{r}_1 \dots \vec{r}_n)}{\prod_{i=1}^n \rho_N^{(1)}(\vec{r}_i)}. \quad (25)$$

The particle distribution functions measure the extent to which the structure of a fluid deviates from complete randomness. If the system is also isotropic, the pair distribution function  $g_N^{(2)}(\vec{r}_1, \vec{r}_2)$  is only a function of the separation,  $r_{12} = |\vec{r}_2 - \vec{r}_1|$ ; it is then usually called the radial distribution function and written simply as  $g(r)$ .

Radial distribution function,  $g(r)$ , and pair correlation function (PCF),  $g(r, \hat{\Omega}_1, \hat{\Omega}_2)$ , are of high importance for the study of simple and molecular liquids, respectively. Wertheim obtained an analytical expression for the distribution function,  $g(r)$  for hard spheres [34]. Boublik calculated a new simple analytical expression for  $g(r)$ , to overcome the difficulties and complexity of the Wertheim function [35]. It is written as

$$g_{\text{Boublik}}(r) = g_1(r) + g_2(r), \quad (26)$$

where

$$g_1(r) = \frac{f(\eta, r)}{1-\eta} \delta(r-1) \delta(r-2), \quad (27)$$

$$g_2(r) = 1 + A \exp(-B(r-r_m)) \cos\left[\frac{\pi}{C}(r-r_m)\right] \delta(r-r_m), \quad (28)$$

with

$$f(\eta, r) = \exp\left[\frac{\eta}{1-\eta} \left(7 - 6r + \frac{r^3}{3}\right) + \dots\right], \quad (29)$$

and

$$C = 2(r_f - 1), \quad (30)$$

where,  $\eta = \rho V$  is the packing fraction,  $r_f$  is the distance for which  $g(r) = 1$ ,  $A = g(r_m - 1)$  and  $B = 1.2(1-\eta)$ .

The value of  $r_m$  can be obtained from

$$\frac{3}{2} \left[ 1 + 3w + w^2 \left( 2 - \frac{\eta}{3} \right) \right] r^2 - \frac{3}{4} w r - \left[ 6 + 9w + \frac{3}{2} w^2 \left( 2 - \frac{\eta}{3} \right) \right] = 0, \quad (31)$$

where  $w = \frac{\eta}{1-\eta}$ . The distance  $r_f$  similarly can be determined from

$$\begin{aligned} & \frac{w}{2} \left[ 1 + 3w + w^2 \left( 2 - \frac{\eta}{3} \right) \right] r^3 - \frac{3}{8} w^2 r^2 \\ & - w \left[ 6 + 9w + \frac{3}{2} w^2 \left( 2 - \frac{\eta}{3} \right) \right] r \\ & + \left[ 7w + \frac{15}{2} w^2 + w^3 \left( 2 - \frac{\eta}{3} \right) - \ln(1-\eta) \right] = 0. \end{aligned} \quad (32)$$

By developing Pynn and Wulf method [36, 37] and using closest approach of Rickayzen [38], and the variational method of Marko [39], along with using Boublik pair distribution, one can obtain a new pair distribution for hard ellipsoidal molecular fluids [40].

$$g_{\text{HE}}(r, \hat{\Omega}_1, \hat{\Omega}_2) = g_{\text{Boublik}} \left( \frac{r}{\sigma(\hat{r}, \hat{\Omega}_1, \hat{\Omega}_2)} \right) \left[ 1 + \alpha P_2(\hat{\Omega}_1, \hat{\Omega}_2) \right], \quad (33)$$

where  $P_2(t) = \frac{1}{2}(3t^2 - 1)$  and  $\sigma = \sigma(\hat{r}, \Omega_1, \Omega_2)$  is the closest approach of Rickayzen [38]. The optimum value of the parameter  $\alpha$  is obtained by the same procedure introduced by Marko. In this method, the error function [39],

$$I(\alpha) = \int d\vec{x} \left\{ 1 + C(\vec{x}, 0) + \rho \int d\vec{x}' C(\vec{x}', 0) [g(\vec{x}, \vec{x}') - 1] \right\}^2, \quad (34)$$

should be minimized with respect to  $\alpha$ .

### 4. Direct correlation function

The direct correlation functions play an important role in the density functional theory [33]. In the DFT, the free energy and the grand potential of a classical system as a functional expansion of one particle density [41, 42] are convenient to study the structural and thermodynamic properties of homogeneous [42] and inhomogeneous fluids [43-45]. The expansion coefficients of the functional are the  $n$ -particle DCF which are the functional derivatives of free energy, as introduced in the

equilibrium state of liquid theory. Here, we intend to consider the pair DCF or simply DCF. In the theory of molecular fluids, the DCF can be used to calculate the equation of state [46], free energy [47], phase transition [39, 48, 49], elastic constants [50], etc. It is generally believed that the repulsive interactions, in particular hard core, are responsible for the main structural features observed in molecular fluids, such as liquid crystals [5]. The DCF,  $C(\vec{r}_1, \vec{r}_2, \rho)$ , of a classical system comprising non-spherical molecules is defined as a second derivative of the grand potential,  $W[\rho]$ ,

$$C(\vec{x}_1, \vec{x}_2, \rho) = -\beta \frac{\delta^2 W[\rho]}{\delta \rho(\vec{x}_1) \delta \rho(\vec{x}_2)} + \frac{\delta(\vec{x}_1 - \vec{x}_2)}{\rho(\vec{x}_1)}, \quad (35)$$

In eq. (35), we have  $\vec{x}_i = (\vec{r}_i, \Omega_i)$ , where  $\vec{r}_i$  and  $\Omega_i$  represent the position and orientation of the molecules, respectively. Another definition of the DCF is given via the OZ equation [33]:

$$h(\vec{x}_1, \vec{x}_2) = C(\vec{x}_1, \vec{x}_2) + \int d\vec{x}_3 \rho(\vec{x}_3) C(\vec{x}_1, \vec{x}_3) h(\vec{x}_3, \vec{x}_2), \quad (36)$$

where  $h(\vec{x}_1, \vec{x}_2)$  is the total correlation function. For short range potential,  $u_{12}(\vec{x}_1, \vec{x}_2)$ , and with the Percus-Yevick (PY) closure, we have

$$C(\vec{x}_1, \vec{x}_2) = [h(\vec{x}_1, \vec{x}_2) + 1] \{1 + \exp[u_{12}(\vec{x}_1, \vec{x}_2)/k_B T]\}^{-1}, \quad (37)$$

The OZ equation can be solved to obtain the correlation functions. The PY analytical solution of OZ equation for the DCF of hard sphere,  $C_{PY}(r)$ , was called PY DCF [51]. Roth *et al.* [52] derived a new expression for the DCF of hard sphere,  $C_{Roth}(r)$ , which is closer to simulation inside the core  $r < d$  than PY approximation. Avazpour and Moradi combined PY and Roth DCF to obtain a new expression for the DCF of hard sphere [40]. This new DCF was in good agreement with the MC simulation [40].

Using the improved Pynn – Wulf [36, 37] expressions proposed by Marko [39] and using the new DCF of ref. [40], the DCF of hard ellipsoids is obtained as:

$$C(r, \Omega_1, \Omega_2) = C_{PY-R} \left( \frac{r}{\sigma(\hat{r}, \Omega_1, \Omega_2)} \right) (1 + \alpha P_2(\Omega_1, \Omega_2)). \quad (38)$$

In this work, the direct correlation function of ref. [39] and Boublik PCF [30] are used to calculate a new direct correlation functions for GB molecular fluids. This new DCF is

$$C(r, \hat{\Omega}_1, \hat{\Omega}_2) = \left[ C_{PY-R} \left( \frac{r}{\sigma(\hat{r}, \hat{\Omega}_1, \hat{\Omega}_2)} \right) \right.$$

$$\left. + f(\vec{r}, \hat{\Omega}_1, \hat{\Omega}_2) g_{Boublik} \left( \frac{r}{\sigma(\hat{r}, \hat{\Omega}_1, \hat{\Omega}_2)} \right) \right] \left[ 1 + \alpha P_2(\hat{\Omega}_1, \hat{\Omega}_2) \right], \quad (39)$$

where  $f(r, \Omega_1, \Omega_2) = \exp[-\beta U(r, \Omega_1, \Omega_2)] - 1$  is the Mayer function,  $\beta = (k_B T)^{-1}$  and  $U(r, \Omega_1, \Omega_2)$  is inter molecular potential.

## 5. Calculation and results

Two methods have been used to study the effect of temperature variation on the isotropic – nematic transition. Firstly, structural parameters have been evaluated numerically. The structural parameters play an important role in the density functional theory and for the study of the temperature dependence of isotropic–nematic transition. The transition density has been obtained from the plot of the structural parameters against reduced density at different reduced temperatures ( $T^* = k_B T / \varepsilon_0$ ). The parameter  $\hat{C}_{00}^0$  is related to the isothermal compressibility while  $\hat{C}_{22}^0$  and higher order coefficients are related to the freezing parameters.

The most commonly used values of GB parameters in the literature are  $k = 3.0$ ;  $k' = 5.0$ ;  $\mu = 2.0$ ;  $\nu = 1.0$  [53]. The  $k$  value was set to be 3, which is the minimum ratio of the length to breadth required, in order to observe liquid crystalline behavior in real systems. The value of reduced temperature  $T^*$  has been varied from 0.8 to 1.2 in steps of 0.05, keeping other parameters fixed at  $k = 3.0$ ;  $k' = 5.0$ ;  $\mu = 2.0$ ;  $\nu = 1.0$ .

The structural parameters of the GB fluid are calculated by using eqs. (1), (17) and (39) with MC integration method. In figures 1 and 2, the structural parameters  $\hat{C}_{ll'}^0$  against  $\rho_f^*(\rho_f^* = \rho_f \sigma_0^3)$  at  $T^* = 0.80$  are compared with the results of ref. [9]. The results of present work are in qualitative agreement with ref. [9]. In figures 3 to 5, we plot the structural parameters  $\hat{C}_{ll'}^0$  at  $T^* = 0.80, 0.95, 1.25$ . It is seen that the values of  $\hat{C}_{ll'}^0$  increase with density and deviate from low-density linear behavior as well as increase steeply near the phase transition. These steep increases can in fact be related to the growth of long-range orientational correlations. Also, as  $T^*$  increases, the phase stability increases toward higher densities and the isotropic–nematic transition takes place at higher densities. In figures. 6 and 7,  $\hat{C}_{22}^0$  and  $\hat{C}_{44}^0$  have been compared at  $T^* = 0.80$  and 1.25. As seen, at all temperatures the structural parameter  $\hat{C}_{22}^0$  is higher than  $\hat{C}_{44}^0$ .

Secondly, the grand thermodynamic potential of system has been used to determine the transition parameters.

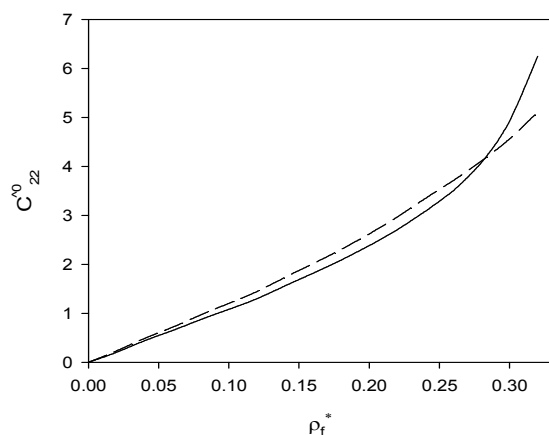


**Figure 1.** The structural parameter  $\hat{C}_{22}^0$  for GB fluid at  $k = 3.0$ ;  $k' = 5.0$ ;  $\mu = 2.0$ ;  $\nu = 1.0$  and  $T^* = 0.80$ . The solid curve is our DCF result and the dashed curve is the results of ref. [9].

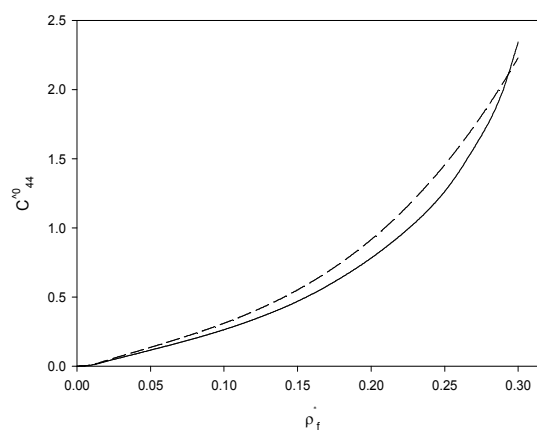


**Figure 2.** The structural parameter  $\hat{C}_{44}^0$  for GB fluid at  $k = 3.0$ ;  $k' = 5.0$ ;  $\mu = 2.0$ ;  $\nu = 1.0$  and  $T^* = 0.80$ . The solid curve is our DCF result and the dashed curve is the results of ref. [9].

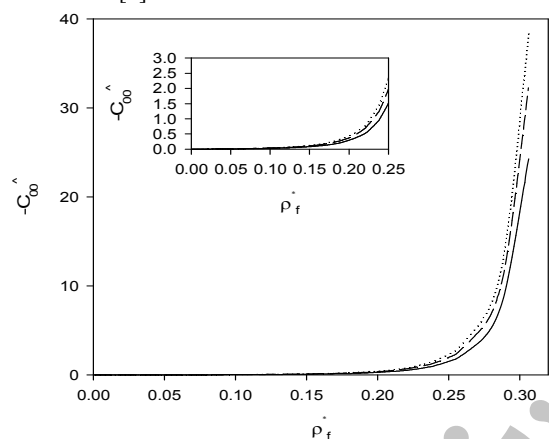


**Figure 3.** The structural parameter  $\hat{C}_{00}^0$  for GB fluid with our DCF at  $k = 3.0$ ;  $k' = 5.0$ ;  $\mu = 2.0$ ;  $\nu = 1.0$ . The curves with solid line, dashed, and dots are for  $T^* = 1.25$ , 0.95, and 0.80, respectively.

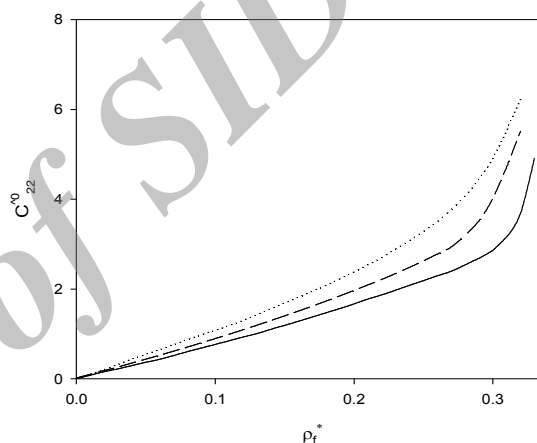


**Figure 4.** Same as figure. 3 but for  $\hat{C}_{22}^0$ .

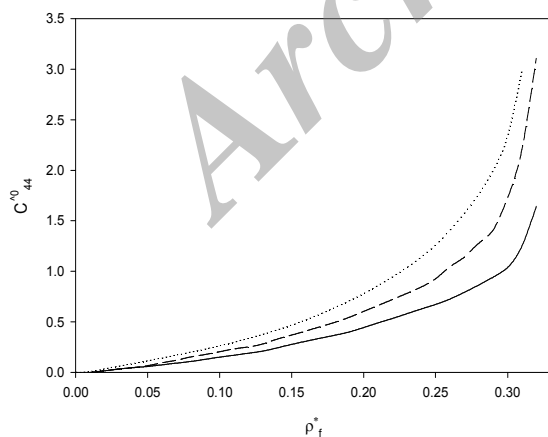


**Figure 5.** Same as figure. 3 but for  $\hat{C}_{44}^0$ .

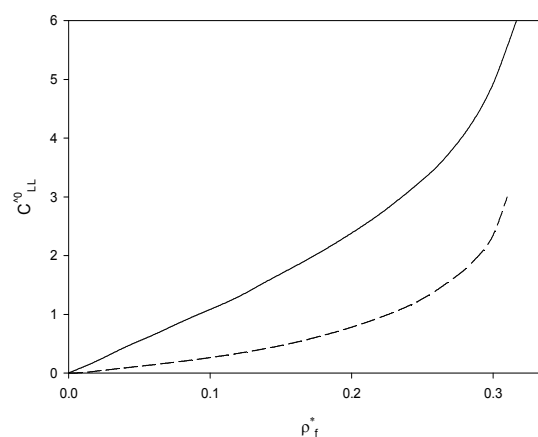


**Figure 6.** The structural parameters  $C_{22}^0$  and  $C_{44}^0$  for GB fluid at  $k = 3.0$ ;  $k' = 5.0$ ;  $\mu = 2.0$ ;  $\nu = 1.0$  and  $T^* = 0.80$ . The solid and the dashed curves are for  $\hat{C}_{22}^0$  and  $\hat{C}_{44}^0$ , respectively.

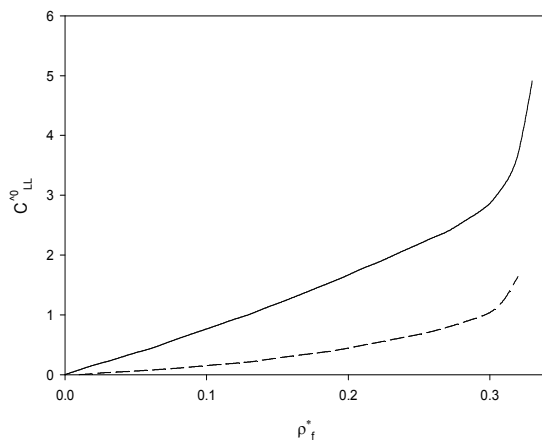


**Figure 7.** Same as figure. 6 but for  $T^* = 1.25$ .

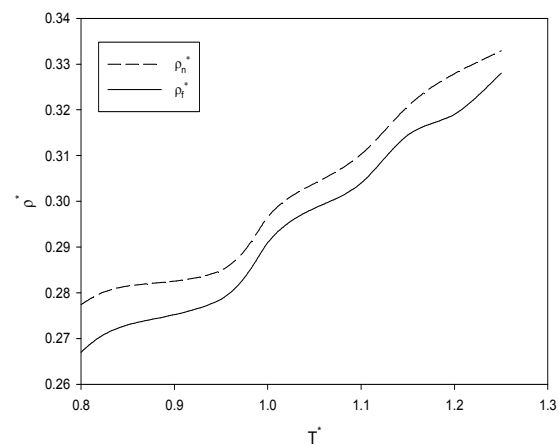


**Figure 8.** The I- N coexistence densities for GB fluid with our DCF at  $k = 3.0$ ;  $k' = 5.0$ ;  $\mu = 2.0$ ;  $\nu = 1.0$ . The curves with solid line and dashed are for  $\rho_f^*$  and  $\rho_n^*$ , respectively.

**Table 1.** Isotropic – nematic transition parameters for GB fluid at  $k = 3.0$ ;  $k' = 5.0$ ;  $\mu = 2.0$ ;  $\nu = 1.0$  and  $0.80 \leq T^* \leq 1.25$ . The structure and other transition parameters are calculated using eq. (39) and DFT method.

| $T^*$ | $\rho_f^*$ | $\rho_n^*$ | $\Delta\rho^*$ | $\bar{P}_2$ | $\bar{P}_4$ | $\hat{C}_{00}^0$ | $\hat{C}_{22}^0$ | $\hat{C}_{44}^0$ |
|-------|------------|------------|----------------|-------------|-------------|------------------|------------------|------------------|
| 0.80  | 0.2670     | 0.2774     | 0.0104         | 0.743       | 0.418       | -1.385           | 3.750            | 1.580            |
| 0.85  | 0.2730     | 0.2815     | 0.0085         | 0.717       | 0.383       | -1.821           | 3.873            | 1.321            |
| 0.95  | 0.2786     | 0.2849     | 0.0063         | 0.690       | 0.350       | -2.741           | 3.910            | 1.277            |
| 1.00  | 0.2910     | 0.2966     | 0.0056         | 0.684       | 0.343       | -2.918           | 4.222            | 1.392            |
| 1.05  | 0.2985     | 0.3039     | 0.0054         | 0.680       | 0.338       | -9.676           | 3.896            | 1.486            |
| 1.10  | 0.3040     | 0.3103     | 0.0063         | 0.679       | 0.337       | -10.339          | 4.206            | 1.483            |
| 1.15  | 0.3145     | 0.3208     | 0.0063         | 0.679       | 0.337       | -18.317          | 4.544            | 1.599            |
| 1.20  | 0.3190     | 0.3279     | 0.0089         | 0.680       | 0.338       | -31.458          | 4.6968           | 1.645            |
| 1.25  | 0.3280     | 0.3329     | 0.0049         | 0.670       | 0.333       | -56.790          | 4.913            | 1.75             |

When the expansion coefficients of the new DCF of the GB fluid are known, we can solve eqs. (20-22). The calculated transition parameters are shown in table 1. The results obtained for transition densities of the GB fluid calculated using the structural parameters and the DFT method are compared in table 2.

As seen in table 1, increasing temperature increases transition densities. Also, second and fourth order parameters decrease with increasing temperature. These increasing and decreasing are consistent with the physics of phase transition. Also comparison of transition densities of table 2, shows correspondence of DFT and structural parameter methods. As figures and tables show, by increasing the temperature, the transition occurs when the structural parameters  $\hat{C}_{22}^0$  and  $\hat{C}_{44}^0$  attain values  $3.750 \leq \hat{C}_{22}^0 \leq 4.913$  and  $1.277 \leq \hat{C}_{44}^0 \leq 1.750$ , respectively. It can be seen that these parameters vary weakly with  $T$ .

In figure. 8, we plot the variation of temperature with isotropic–nematic coexistence densities ( $\rho^*$ ), found from the density-functional theory. The theoretical results show that the coexistence densities  $\rho_f^*$  and  $\rho_n^*$  increase with increasing temperature. The fractional density changes,  $\Delta\rho^*$ , are also found to be rather small, which is consistent with the fact that the molecules are hard and not very compressible at the transition densities. As seen in figures 1 and 2, our DCF gives reasonable results for the structural parameters. However, it quantitatively underestimates the structural parameters of ref. [9]. Hence, as Singh *et al.* [9] emphasized, the phase transitions in complex fluids can be predicted reasonably well with the density-functional method if the values of the DCFs in the isotropic phase are accurately known. In addition, our new DCF is convenient for the study of other physical properties of

**Table 2.** Comparison of the calculated transition densities,  $\rho_f^*$ , for GB fluid at  $k = 3.0$ ;  $k' = 5.0$ ;  $\mu = 2.0$ ;  $\nu = 1.0$  and  $0.80 \leq T^* \leq 1.25$ , using DFT and structural parameters.

| $T^*$ | Transition density $\rho_f^*$ | Transition density $\rho_f^*$ from |
|-------|-------------------------------|------------------------------------|
|       | from DFT                      | structure parameters               |
| 0.80  | 0.2670                        | 0.2700                             |
| 0.85  | 0.2730                        | 0.2780                             |
| 0.95  | 0.2786                        | 0.2870                             |
| 1.00  | 0.2910                        | 0.2965                             |
| 1.05  | 0.2985                        | 0.3050                             |
| 1.10  | 0.3040                        | 0.3180                             |
| 1.15  | 0.3145                        | 0.3205                             |
| 1.20  | 0.3190                        | 0.32650                            |
| 1.25  | 0.3280                        | 0.3310                             |

GB liquid crystals. From the results tabulated and graphed, it is obvious that the DFT with our DCF provides a good description of the I-N phase transition of GB fluids. Also, the DFT calculations of GB fluids have shown that the temperature and DCF can have a profound influence on the phase behavior.

### Acknowledgments

The authors would like to thank Research Council, Yasouj University, for partial financial support.

### References

1. S Singh, "Liquid crystals: fundamentals", World Scientific (2002).
2. P G de Gennes and J Prost, "The Physics of Liquid Crystals", Clarendon Press, Oxford (1993).
3. S Chandrasekhar, "Liquid Crystals", Cambridge Univ. Press, Cambridge (1992).
4. I G Kaplan, "Intermolecular Interactions: Physical Picture, Computational Methods and Model Potentials", John Wiley and Sons, Ltd. (2006).
5. C G Gray and K E Gubbins, "Theory of Molecular Fluids Fundamental", Oxford University, New York (1984).
6. B J Berne and P Pechukas, *J. Chem. Phys.* **56** (1972) 4213.
7. J G Gay and B J Berne, *J. Chem. Phys.* **74** (1981) 3316.
8. R C Singh, *Mol. Cryst. Liq. Cryst.* **457** (2006) 67.
9. R C Singh, *J. Phys.: Condens. Matt.* **19** (2007) 376101.
10. G R Luckhurst, R A Stephens, and R W Phippen, *Liq. Cryst.* **8** (1990) 451.
11. G R Luckhurst and K A Satoh, *Mole. Cryst. and Liq. Cryst.* **402** (2003) 321.
12. M A Bates and G R Luckhurst, *J. Chem. Phys.* **110** (1999) 7087.
13. J S Lintuvuori and M R Wilson, *J. Chem. Phys.* **128** (2008) 044906.
14. R Berardi *et al.*, *J. Chem. Phys.* **131** (2009) 174107.
15. R Berardi *et al.*, *J. Chem. Phys.* **135** (2011) 134119.
16. E Velasco, A M Somoza, and L Mederos, *J. Chem. Phys.* **102** (1995) 8107.
17. V V Ginzburg, M A Glaser, and N A Clark, *Liq. Cryst.* **21** (1996) 265.
18. R C Singh, J Ram, and Y Singh, *Phys. Rev. E* **54** (1996) 977.
19. R C Singh and J Ram, *Physica A* **326** (2003) 13.
20. Y Singh, *Phys. Rep.* **207** (1991) 351.
21. D L Cheung and F Schmid, *J. Chem. Phys.* **120** (2004) 9185.
22. M Moradi and A Avazpour, *Iranian J. Phys. Res.* **4**, 3 (2004) 267.
23. J Alejandro, J W Emsley, and D J Tildesley, *J. Chem. Phys.* **101** (1994) 7027.
24. M P Allen, M A Warren, and M R Wilson, *et al.*, *J. Chem. Phys.* **105** (1996) 2850.
25. J Stelzer, L Longa and H R Trebin, *J. Chem. Phys.* **103** (1995) 3098.
26. S Sarman and D J Evans, *J. Chem. Phys.* **99** (1993) 9021.
27. S Sarman, *J. Chem. Phys.* **101** (1994) 480.
28. S Sarman and D J Evans, *J. Chem. Phys.* **99** (1993) 620.
29. S Sarman, *J. Chem. Phys.* **103** (1995) 393.
30. E de Miguel, L F Rull and K E Gubbins, *Phys. Rev. A* **45** (1992) 3813.
31. R C Singh, J Ram and Y Singh, *Phys. Rev. E* **65** (2002) 031711.
32. S Singh, *Phys. Rep.* **324** (2000) 107.
33. J P Hansen and I R McDonald, "Theory of Simple Liquids," Academic, London (1976).



34. M S Wertheim, *Phys. Rev. Lett.* **10** (1963) 321.
35. T Boublik, *Mol. Phys.* **91** (1997) 161.
36. R Pynn, *J. Chem. Phys.* **60** (1974) 4579.
37. A Wulf, *J. Chem. Phys.* **67** (1977) 2254.
38. G Rickayzen, *Mol. Phys.* **98** (1998) 393.
39. J F Marko, *Phys. Rev. Lett.* **60** (1988) 325.
40. A Avazpour and M Moradi, *Physica B* **392** (2007) 242.
41. C Ebner, H R Krishnamurthy and R Pandit, *Phys. Rev. A.* **43** (1991) 4355.
42. M Moradi and H Shahri, , *Iranian J. Phys. Res.* **3**, 4 (2003) 275.
43. R Evans, in: D. Henderson (Ed.), “*Inhomogenous Fluids*”, Dekker, New York (1992).
44. M Moradi, R J Wheatley, and A Avazpour, *J. Phys.: Cond. Matt.* **17** (2005) 5625.
45. M Moradi, R J Wheatley, and A Avazpour, *Phys. Rev. E.* **72** (2005) 061706.
46. E de Migule and E M del Rio, *J. Chem. Phys.* **118** (2003) 1852.
47. A Gonzalez and J A White, *Physica A* **296** (2001) 347.
48. M Baus, J L Colot, and X G Wu, *et al.*, *Phys. Rev. Lett.* **59** (1987) 2184.
49. J A Cuesta, C F Tejero, and M Baus, *Phys. Rev. A* **39** (1989) 6498.
50. N H Phuong, G Germano, and F Schmid, *J. Chem. Phys.* **115** (2001) 7227.
51. W R Smith and D Handerson, *Mol. Phys.* **3** (1970) 411.
52. R Roth, R Evans, and A Long, *et al.*, *J. Phys.: Cond. Matt.* **14** (2002) 12063.
53. P Mishra and J Ram, *Eur. Phys. J. E* **14** (2005) 345.

Archive of SID